Eur. J. Mineral.
2009, **21**, 251–260

Nechelyustovite, a new heterophyllosilicate mineral, and new data on bykovaite: a comparative TEM study

PÈTER NÈMETH[1, 4], ALEXANDER P. KHOMYAKOV[2], GIOVANNI FERRARIS[1, *] and YURIY P. MENSHIKOV[3]

[1]Dipartimento di Scienze Mineralogiche e Petrologiche, Università di Torino,
Via Valperga Caluso 35, 10125 Torino, Italy
*Corresponding author, e-mail: giovanni.ferraris@unito.it
[2]Institute of Mineralogy, Geochemistry and Crystal Chemistry of Rare Elements,
Veresaev Street 15, Moscow 121357, Russia
[3]Geological Institute Kola Science Centre of Russian Academy of Science, Fersman Street 14,
Apatity 184200, Russia
[4]Present address: Chemical Research Center of the Hungarian Academy of Sciences, Pusztaszeri út 59-67,
Budapest 1025, Hungary

Abstract: A new mineral species, nechelyustovite, $(Ba_{0.75}Sr_{0.25}K_{0.17}Ce_{0.02}Ca_{0.01}\square_{0.80})_{\sum 2.00}\{(Na_{2.20}Ti_{0.94}Mn_{0.62}Ca_{0.20}Fe_{0.04})_{\sum 4.00}[(Ti_{1.33}Nb_{0.67})_{\sum 2.00}O_2Si_4O_{14}](O_{1.30}H_2O_{0.70})_{\sum 2.00}\}\cdot 4.325H_2O$ (electron microprobe), was collected from a hydrothermally altered pegmatite body emplaced in the nepheline syenites near their contact with ijolite–urtites in the south-western part of the Khibiny alkaline massif, Kola Peninsula, Russia, in the underground Kirovskii Mine at Mount Kukisvumchorr. It forms rosettes scattered in a natrolite matrix which are up to 1–5 cm in diameter and composed of extremely fine (0.01–0.1 mm) bounded flakes and lamellae. Nechelyustovite is associated with natrolite, belovite-(La), belovite-(Ce), gaidonnayite, nenadkevichite, epididymite, fluorapophyllite, sphalerite and submicrometric barytolamprophyllite. It is creamy with greyish, bluish or yellowish shades; streak is white, lustre vitreous, pearly or silvery; translucent, transparent in fine flakes formed by [010] elongated and (001) flattened lamellae; $H = 3$ (Mohs); {001} perfect and {100} medium cleavages; brittle; fracture uneven; $D_{meas} = 3.32–3.42(2)$, $D_{calc} = 3.22$ g/cm^3. Biaxial (+); at 589 nm $\alpha = 1.700(3)$, $\beta = 1.710(3)$, $\gamma = 1.734(3)$; 2V(calc) 66°; $X \sim c$, $Y \sim a$, $Z \sim b$. Nechelyustovite, simplified as $(Ba,Sr,K,\square)_2\{(Na,Ti,Mn)_4[(Ti,Nb)_2O_2Si_4O_{14}](O,H_2O,F)_2\}\cdot 4.5H_2O$, is a new heterophyllosilicate member of the mero-plesiotype bafertisite series and a transmission electron microscopy (TEM) study shows that it occurs as two polytypes intergrown at submicrometric scale: polytype 1*M*, *P*2/*m*, $a = 5.37$, $b = 7.00$, $c = 24.05$ Å, $\beta = 91.1°$, $Z = 2$; polytype 2*M*, *A*2/*m*, $a = 5.38$, $b = 7.04$, $c = 48.10$ Å, $\beta = 91.1°$, $Z = 4$. The spacing (Å) and intensities of the most intense X-ray powder diffraction peaks are 24.06 (100), 7.05 (13), 5.95 (36), 3.95 (25), 2.828 (42), 2.712 (19) and 2.155 (13). A TEM study of bykovaite, simplified as $(Ba,Na,K,\square)_2\{(Na,Ti,Mn)_4[(Ti,Nb)_2O_2Si_4O_{14}](H_2O,F,OH)_2\}\cdot 3.5H_2O$, shows that also this heterophyllosilicate occurs as two polytypes intergrown at submicrometric scale: polytype 1*M*, *P*112/*m*, $a = 5.552$, $b = 7.179$, $c = 25.47$ Å, $\gamma = 91.1°$, $Z = 2$; polytype 2*M*, *I*112/*m*, $a = 5.552$, $b = 7.179$, $c = 50.94$ Å, $\gamma = 91.1°$, $Z = 4$. Hypotheses on the crystal structure of the two minerals are discussed.

Key-words: new mineral species, nechelyustovite, bykovaite, heterophyllosilicates, Khibiny massif, Kola Peninsula, TEM study.

Introduction

Agpaitic nepheline syenites with hyperagpaitic pegmatites and hydrothermalites which occur in the Khibiny and Lovozero massifs, Kola Peninsula, Russia, are the products of extremely alkaline conditions of mineral formation in magmatic processes (Khomyakov, 1995). Together, these massifs constitute the gigantic, about 2000 km^2, Khibiny–Lovozero complex (Pekov, 2000; Yakovenchuk *et al.*, 2005) representing a unique natural laboratory. There the overall list of minerals has reached more than 600 entries, half of which are endemic to agpaitic nepheline syenites (above 100 of them are unknown outside this complex) and about 200 have been described as new species (Khomyakov, 2008). In this complex, more than 50 % of minerals are silicates, with about 1/3 of the latter being titano-, niobo- and zircono-silicates.

From the hyperalkaline rocks of Kola Peninsula, Khomyakov (1995) reported partial descriptions of several unknown species and listed them as Mnn phases (M stands for mineral and nn is a two-digit identifying number). Often the delay to fully characterize Mnn phases was due to the lack of single crystals suitable for an X-ray diffraction study. In recent years, applying electron microscopy and the concepts of the modular crystallography (Ferraris *et al.*, 2008), some Mnn phases, have been either identified as new mineral species [seidite-(Ce) (M31; Khomyakov *et al.*, 1998; Ferraris *et al.*, 2003); nafertisite (M71;

0935-1221/09/0021-1864 $ 4.50
DOI: 10.1127/0935-1221/2009/0021-1864

Khomyakov *et al.*, 1995; Ferraris *et al.*, 1996); bykovaite (M72; Khomyakov *et al.*, 2005)] or better characterized [M51, M55 and M75 (shkatulkalite); Nèmeth, 2004].

A part of the Mnn phases can be characterized by a phyllosilicate *TOT*-like layer, in which rows of *X* (mainly Ti, Nb and Zr) polyhedra substitute rows of the disilicate tetrahedra in the *T* sheets. These minerals were named as heterophyllosilicates (Ferraris *et al.*, 1996; Ferraris, 1997) and their structures are based on *HOH* layers (*H* stands for *hetero* to indicate the presence of the *X* heteropolyhedra alternated to silicate tetrahedra). As summarized by Ferraris (1997), depending on the periodicity of the substitution, three types of *HOH* layers are known: bafertisite-, astrophyllite- and nafertisite-type. Actually, each type of *HOH* layer can be further differentiated if the position of the two *H* sheets relatively to the *O* sheet is analyzed as shown by Zvyagin & Vrublevskaya (1976) for astrophyllite and Ferraris *et al.* (1996) for nafertisite; the bafertisite type is discussed below.

The heterophyllosilicates form a B_1M_n polysomatic series which is based on *B* (bafertisite-type) and *M* (mica-type) modules; a recent review is in Ferraris (2008). The members with $n = 0$ have general formula $A_2\{Y_4[X_2(O')_{2+p}Si_4O_{14}](O'')_2\}W$. In this formula, atoms belonging to the *H* sheet only and the *HOH* layer are shown in the square brackets and braces, respectively; *A* (cations) and *W* (anions and H_2O) represent the interlayer content; *Y* and *X* are cations in the *O* and *H* sheets, respectively; O′ (bonded to *X*) and O″ (belonging to the octahedral *O* sheet only) can be oxygen, hydroxyl, fluorine or water molecules. The value of *p* depends on the co-ordination of the *X* cation. If this cation is octahedrally co-ordinated, the sixth corner of the polyhedron can be (i) unshared ($p = 2$), (ii) shared with a second *X* octahedron ($p = 1$) or (iii) with an anion of an interlayer polyhedron ($p = 0$); $p = 0$ holds also when *X* is five-fold coordinated.

About 30 different mineral species correspond to the member with $n = 0$ of the heterophyllosilicate series and form the mero-plesiotype bafertisite series (Ferraris *et al.*, 2001; 2008) where each member has a different interlayer content (merotypy; Makovicky, 1997), and the configuration of the *HOH* layer may be modified (plesiotypy; Makovicky, 1997). Extending a first analysis by Christiansen *et al.* (1999), Sokolova (2006) classifies the following topologies that occur in the so-called bafertisite-type *HOH* layer: (i) the *O* sheet is a pseudo-mirror plane for its two adjacent *H* sheets (linkage 1); the two *H* sheets show a relative displacement which is either (ii) *b*/2 (linkage 2) or (iii) a compromise between (i) and (ii).

Based mainly on transmission electron microscope (TEM) data, this paper reports the description of the new species nechelyustovite and new data on the crystal-chemically related species bykovaite (Khomyakov *et al.*, 2005). Nechelyustovite was discovered in the Khibiny massif about 20 years ago and listed by Khomyakov (1995) as Ba-bearing titano-niobosilicate M73; however, its characterization could not be completed for lack of crystallographic data. The mineral species and name were approved by the Commission on New Minerals, Nomenclature and Classification, International Mineralogical Association (IMA 2006-021); the name honours Georgii N. Nechelyustov (born in 1939), a noted Russian electron microprobe analyst of new mineral species, in particular titano-silicates. Type material is deposited at the Fersman Mineralogical Museum, Russian Academy of Sciences, Leninskii Pr. 18/2, 117071 Moscow, Russia (catalogue number 3437/1).

Experimental details

Samples of the new mineral nechelyustovite and revised bykovaite were investigated by a Specord 75 IR spectrophotometer (sample in KBr pellet), a Philips CM12 TEM (LaB6 filament, operated at 120 kV), an X'Pert X-ray powder diffractometer (Bragg-Brentano geometry, Cu*K*α radiation, graphite monochromator) and an ARL-SEMQ electron-microprobe instrument (wavelength-dispersion mode; 15 kV and 30 nA; beam diameter 10 μm). Selected area electron diffraction (SAED) patterns were obtained on crushed grains. Nechelyustovite was also oriented perpendicular to the (001) lamellae and then thinned by using a Technoorg-Linda ion-beam thinner (accelerating voltage 5 keV, milling angle 8°). The cell parameters of the two nechelyustovite and bykovaite polytypes were obtained by the Unit Cell program (Holland & Redfern, 1997) and GSAS software (http://www.ccp14.ac.uk/ccp/ccp14/ftp-mirror/gsas/public/gsas/), respectively.

Occurrence and physical properties

Nechelyustovite

Except data originally collected by the author A.P.K. (including IR-spectra) (Khomyakov, 1995) on a small quantity of quite pure nechelyustovite selected from the type material, data first given in this paper (TEM, X-ray powder diffraction (XRPD) and new chemical analysis) have been obtained from the remaining sample, as shown by the back-scattered electron (BSE) image (Fig. 1) and SAED patterns described below. In Fig. 1 the new mineral is strictly associated, even at submicrometric scale, with natrolite and barytolamprophyllite; the latter cannot be optically identified. In the BSE image, nechelyustovite can be distinguished by its higher scattering factor of heavy atoms (Ba, Nb, *etc.*) with respect to natrolite.

Nechelyustovite occurs in the south-western part of the Khibiny alkaline massif, Kola Peninsula, Russia, in the underground Kirovskii Mine (+252 m level) at Mount Kukisvumchorr. The type specimens were collected by A.P.K. and Yu. P.M. in 1989 from a hydrothermally altered pegmatite body emplaced in the nepheline syenites near their contact with ijolite–urtites. The pegmatite is a branching vein 0.1–0.5 m wide with a lens-like swell of symmetrical zoned structure. It consists of a natrolite core, a microcline zone surrounding the core and a marginal aegirine-dominated zone with subordinate amounts of microcline, nepheline, lamprophyllite and eudialyte. Nechelyustovite is confined to the natrolite core, where it forms rosettes up to 1–5 cm in diameter composed of extremely fine (0.01–0.1 mm) bounded flakes and lamellae. In the core, most rosettes are scattered in natrolite, some

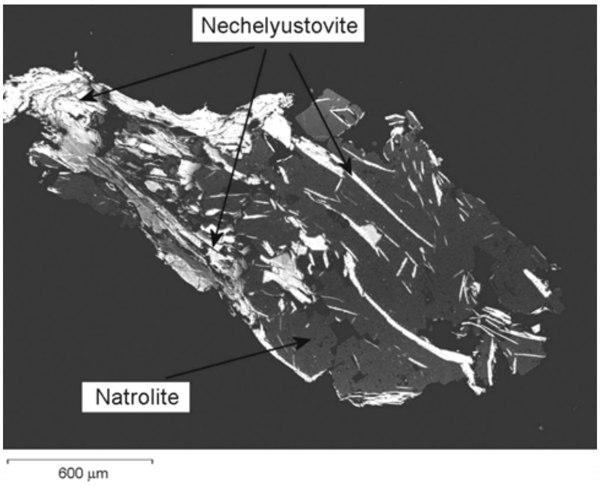

Fig. 1. Back-scattered electron (BSE) image of nechelyustovite (light grey) in a matrix of natrolite (dark grey).

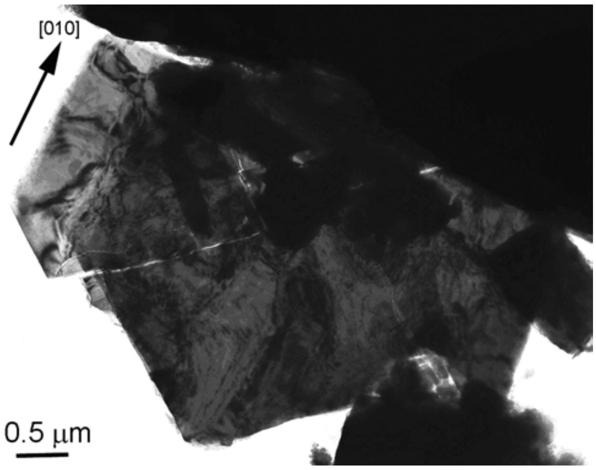

Fig. 2. TEM image showing lamellae of nechelyustovite.

are instead in a matrix of carbonate-hydroxylapatite. Other associated minerals are: belovite-(La), belovite-(Ce), gaidonnayite, nenadkevichite, epididymite, fluorapophyllite, sphalerite and submicrometric barytolamprophyllite. According to Pekov & Podlesnyi (2004), the full list of minerals found in this pegmatite body (number 2 in their work), which has grown to 24 entries in recent years, includes such rare species as manganokukisvumite and Na-komarovite.

As revealed by the electron diffraction study further discussed below, nechelyustovite consists of two polytypes which are intergrown on submicrometric scale. Consequently, all the macroscopic properties here reported refer to both polytypes. Nechelyustovite is creamy with greyish, bluish or yellowish shades; streak is white, lustre vitreous, pearly or silvery; translucent, transparent in fine flakes; fluorescence is absent with UV in the range 240–400 nm; $H = 3$ (Mohs); {001} perfect and {100} medium cleavages; brittle; fracture uneven; parting is not observed. The measured and calculated densities are 3.32–3.42(2) (volumetric method) and 3.20 g/cm^3 (average value for two compositions; see below), respectively. Biaxial (+); at 589 nm $\alpha = 1.700(3)$, $\beta = 1.710(3)$, $\gamma = 1.734(3)$; 2V(calc) 66°; dispersion is not discernible; optically pseudo-orthorhombic; $X \sim c$, $Y \sim a$, $Z \sim b$; pleochroism is not discernible; fibres are elongated along the *b* axis and (001) flattened (Fig. 2). The compatibility according to Mandarino (1981) is 0.106 (poor); taking into account the data for TiO_2 refraction in bafertisite-like heterophyllosilicates by Perekalina & Khomyakov (1999), the compatibility is 0.008 (superior).

The band at 3410 cm^{-1} in the infrared spectrum of nechelyustovite (Table 1) shows the presence of H_2O in the mineral structure. The amount of H_2O could not be determined directly but only by difference to 100 % of the electron microprobe chemical data (see below).

Bykovaite

Data reported here are taken from Khomyakov *et al.* (2005). Bykovaite [listed as M72 by Khomyakov (1995)] was discovered in the lenticular pegmatite Shkatulka that occurs at Mount Alluaiv in the northwest part of the Lovozero alkaline massif, Kola Peninsula, Russia. It occurs as creamy or pale yellow compact spheres, up to 3–5 mm in diameter, and spherical aggregates of extremely tiny (0.005–0.05 mm) fibres radiating from a common centre. Bykovaite is associated with bornemanite, labuntsovite and the following minerals: ussingite, potassium feldspar, aegirine, riebeckite, vuonnemite, shkatulkalite, lomonosovite, steenstrupine-(Ce), belovite-(Ce), sidorenkite, terskite, chkalovite, tugtupite, litvinskite, polylithionite, serandite, makatite and sphalerite.

The mineral is biaxial (+), and has refractive indices: $\alpha = 1.668(2)$, $\beta = 1.679(2)$, $\gamma = 1.710(2)$ (589 nm); 2V (meas) = 63(5)° and 2V (calc) = 63°. The orientation is: $a \sim Y$, $b \sim Z$, $c \sim X$. [010] fibres are (001) flattened. It has prefect {001} and good {100} cleavages. The hardness on Mohs scale is 3. The density was measured by volumetric method and gave 2.98 g/cm^3.

The band at 3420 cm^{-1} in the infrared spectrum (Table 1) confirms the presence in the mineral structure of H_2O whose amount corresponds to a 10 % weight loss in the range 20–980° determined by thermal analysis. In this range of temperature, clear endothermic effects at 180, 840, 880 and 960 °C correspond to successive dehydration and incongruent melting of bykovaite.

Transmission electron microscopy study

TEM observation of the crushed grains reveals that both nechelyustovite and bykovaite consist of thin lamellae (about 10–20 nm thick) that show a perfect {001} cleavage. A definite [010] elongation is observed for nechelyustovite (Fig. 2). The samples are strongly electron beam sensitive, but SAED patterns could be obtained. Generally, their qualities are poor (both from the degradation under the electron beam and the poor crystallinity), but they could be used to determine the cell parameters and the space groups of two polytypes in both nechelyustovite and bykovaite.

Table 1. Absorption bands in the IR-spectra of nechelyustovite (1), bykovaite (2) and bornemanite (3) (sh = shoulder; s, m, w = strong, medium and weak bands).

Frequency, cm^{-1}	3500	3000	1600	1100	1000	900	800	600	500	400
1	–	3410m	1616w	–	1046s	985sh 946s 907s	843s	685w	548s 500w	454s
2	–	3420m	1655m	–	1050m	945s	890s 870sh	683w	555m	460m 407m
3	3520w	3390w 3230w	1620w	1101sh	1063s 1011s	980s 958s 943s	836s	684w	595sh 580sh 561m 548s 520sh 500sh	455m 400s

Note. 1 – Khibiny, Mt Kukisvumchorr (this work); 2 – Lovozero, Mt Alluaiv (Khomyakov *et al.*, 2005); 3 – Lovozero, Mt Karnasurt (personal collection of the author A.P.K.).

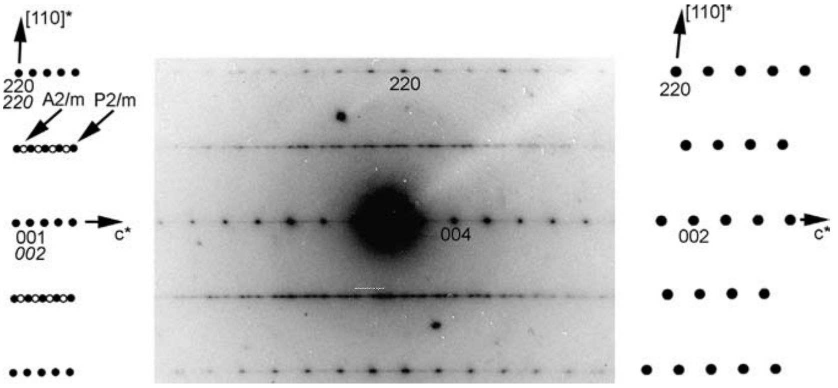

Fig. 3. SAED pattern of barytolamprophyllite intergrown with the polytypes *P*2/*m* and *A*2/*m* of nechelyustovite; the direction of the incident beam is [1$\bar{1}$0] for all phases. The right side of the figure shows the contribution of barytolamprophyllite; the left side of the figure shows the contributions of the *P*2/*m* (filled circles) and *A*2/*m* (open circles) polytypes, respectively; the indices of the latter are in italics. The reflections of the two polytypes overlap for *k* and *l* = 2*n*.

Nechelyustovite

The observed grains of nechelyustovite consist of domains of two monoclinic polytypes; besides, both polytypes are affected by the presence of oriented modules of a lamprophyllite group mineral (Fig. 3). Based on XRPD measurement (see below) probably it corresponds to barytolamprophyllite (*a* = 5.393, *b* = 7.089, *c* = 19.833 Å, β = 96.66°, space group *A*2/*m*; Peng *et al.*, 1984). The size of the domains can be even smaller than that of the selected area aperture (0.2 μm), such that diffractions from both polytypes appear on the same SAED. The identifications of different phases are possible due to the differences either between the space groups (two polytypes of nechelyustovite) or between the cell parameters (nechelyustovite and barytolamprophyllite). The contribution of nechelyustovite to the SAED patterns shown in Fig. 4a and 5a can be indexed on the basis of a polytype 1*M* with cell parameters *a* ~ 5.4, *b* ~ 7.0, *c* ~ 24 Å, β ~ 91° and space group *P*2/*m* (or *Pm*). The SAED patterns of Fig. 4b and 5b show instead a polytype 2*M* with cell parameters *a* ~ 5.4, *b* ~ 7.0, *c* ~ 48 Å, β ~ 91° and space group *A*2/*m* (or *Am*). However, the superposition of the polytype 2*M* on the polytype 1*M* cannot be excluded for Fig. 4a, because the reflections of the polytypes overlap for *k* and *l* = 2*n*. Comparison of the cell parameters, in particular *a* ~ 5.4 and *b* ~ 7.0 Å, with those (*a* = 5.552, *b* = 7.179, *c* = 50.94 Å, γ = 91.10°) given by Khomyakov *et al.* (2005) for bykovaite and chemical composition suggests that nechelyustovite is a member of the bafertisite series (see section Discussion). For this reason, the non-standard orientation *A*2/*m* is adopted to have the *c* parameter stacking the heterophyllosilicate *HOH* layer whose basic periodicities are *a* ~ 5.4 and *b* ~ 7.0 Å.

Bykovaite

The occurrence of two polytypes in nechelyustovite suggested a TEM reinvestigation of bykovaite which too turned out to consist of two polytypes on the basis of the following experimental data. The SAED pattern along [001] can be indexed on the basis of a *P* lattice with cell parameters *a* ~ 5.5, *b* ~ 7.1 Å and γ ~ 91° (Fig. 6). However, it shows systematically stronger reflections for *h* + *k* = 2*n* that

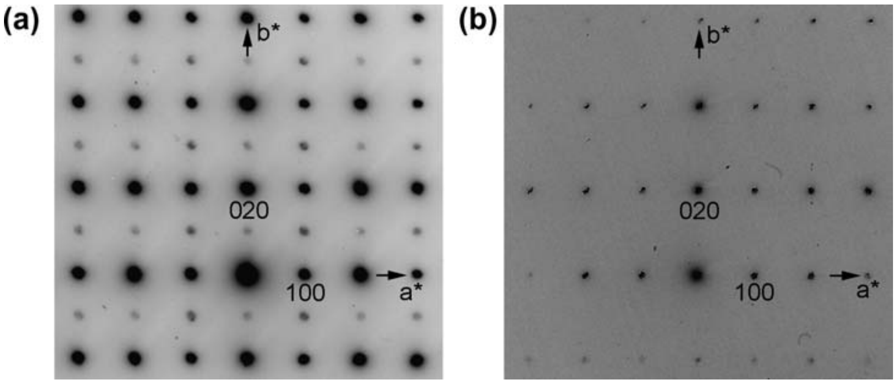

Fig. 4. SAED patterns along [001] obtained from two different grains of nechelyustovite show two different polytypes. (a) *P*2/*m* with $a \sim 5.4$ Å and $b \sim 7.0$ Å; (b) *A*2/*m* with $a \sim 5.4$ Å and $b \sim 7.0/2 = 3.5$ Å because of systematic absences for $k = 2n + 1$.

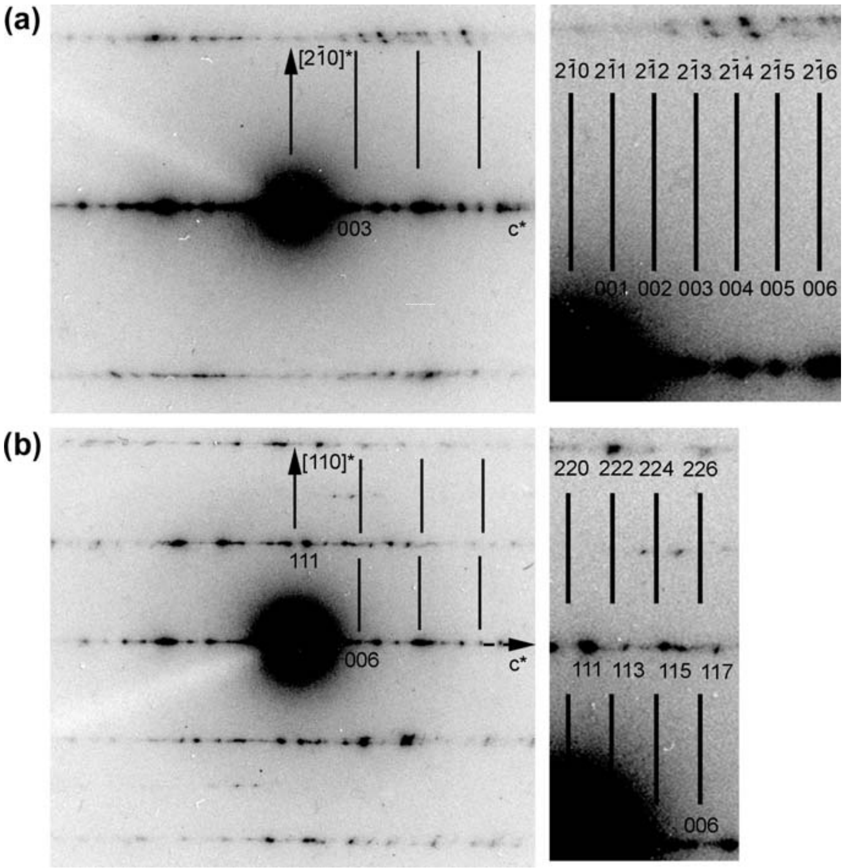

Fig. 5. SAED patterns of nechelyustovite: (a) *P*2/*m* polytype along [120]; (b) *A*2/*m* polytype along [1$\bar{1}$0]. Black lines reveal weak reflections for $k + l = 2n + 1$ (a) and systematic absences for $k + l = 2n + 1$ (b), respectively. Enlarged areas at the right side of the patterns show reflections and reveal possible systematic absences for identifying the two polytypes.

belong to an *I* centred lattice with the same *a*, *b* and γ cell parameters of the *P* lattice. The SAED patterns along [010], [100] and [2$\bar{1}$0] show that they can be indexed on the basis of the *a*, *b* and γ cell parameters given above with $c \sim 25$ and ~ 50 Å for a *P* (Fig. 7) and *I* (Fig. 8) centred lattice, respectively. Broad, elongated reflections close to discrete ones along *c** indicate stacking faults. The domains of samples originating the two types of diffraction patterns are intergrown, as shown by their simultaneous diffraction in most SAED patterns. The two types of domains do not differ in chemical composition, thus the description of the species given by Khomyakov *et al.* (2005) remains valid and represents the average data which can be obtained from the available samples of bykovaite. The present results show

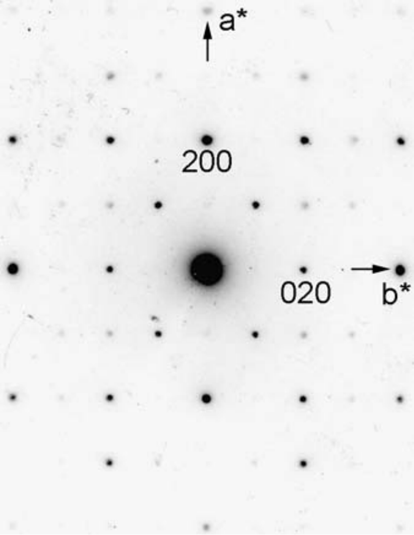

Fig. 6. SAED pattern of bykovaite along [001].

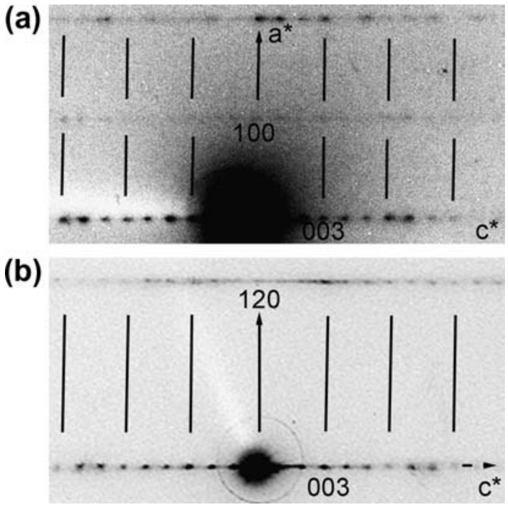

Fig. 7. SAED patterns of bykovaite 1*M* polytype (*P* lattice) along [010] (a) and [2$\bar{1}$0] (b). Black lines reveal weak reflections for $h + k + l = 2n + 1$.

however that this species occurs as two monoclinic polytypes (bykovaite-1*M* and bykovaite-2*M*) to which space groups *P*112/*m* (or *P*11*m*) and *I*112/*m* (or *I*11*m*) are assigned on the basis of the TEM data. The non-standard space groups are adopted for the same reason given for nechelyustovite.

X-ray powder diffraction and cell parameters

Nechelyustovite

The presence of nechelyustovite in the XRPD pattern of the best available sample (Fig. 1) is only of the order of some percent; the rest is represented by major natrolite and minor barytolamprophyllite (Fig. 9). In addition, the low crystallinity due to stacking faults in the polytypic sequences and a strong effect of preferential orientation result in very poor XRPD patterns with broad peaks. Thus, starting from approximate values obtained from electron diffraction for nechelyustovite and the known parameters of natrolite and barytolamprophyllite the D_{obs} given in Table 2 were extracted and used to obtain the following values of the cell parameters of the two nechelyustovite polytypes: $a = 5.37(2)$, $b = 7.00(2)$, $c = 24.05(2)$ Å, $\beta = 91.1(4)°$ for the polytype 1*M*; $a = 5.38(2)$, $b = 7.04(2)$, $c = 48.10(6)$ Å, $\beta = 91.1(4)°$ for the polytype 2*M*.

Bykovaite

Similar to nechelyustovite, low crystallinity due to stacking faults in the polytypic sequences results in very poor X-ray diffraction pattern with high background and broad peaks (Fig. 10). In addition to the two polytypes 1*M* and 2*M*, a labuntsovite group mineral (L) is also present in the XRPD pattern. Therefore, only the cell parameters of the *P*112/*m* polytype [$a = 5.552(1)$, $b = 7.179(1)$, $c = 25.47(1)$ Å, $\gamma = 91.10(1)°$] could be optimized by the cell-refinement module implemented in GSAS software package. The cell parameters of the *I*112/*m* polytype can be obtained using the same *a* (5.552 Å), *b* (7.179 Å), γ (91.10°) values given above, and doubling the *c* (50.94 Å) value.

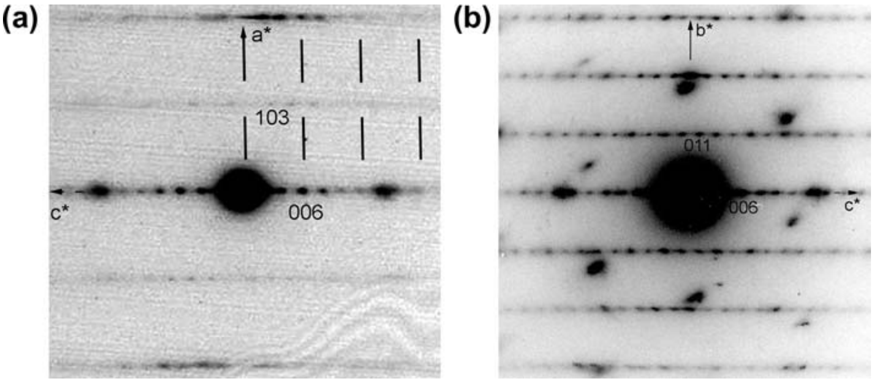

Fig. 8. SAED patterns of bykovaite 2*M* polytype (*I* lattice) along [010] (a) [taken by I. Dódony using a JEOL JEM 4000EX TEM (400 kV; LaB6 filament, top-entry, double-tilt stage; $C_s = 1$ mm; point resolution 1.6 Å)] and [100] (b). Black lines reveal systematic absences for $h + k + l = 2n + 1$.

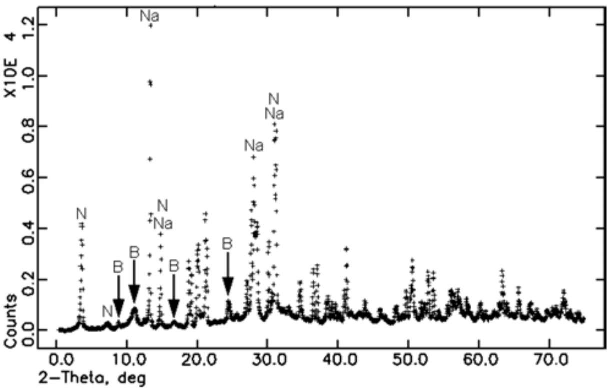

Fig. 9. Observed XRPD pattern of nechelyustovite (N). The most intense peaks of natrolite and barytolamprophyllite are labelled Na and B, respectively.

Crystal-chemical formulae

Nechelyustovite

Table 3 shows the chemical data obtained in this work and those published by Khomyakov (1995) (Superprobe-733 electron-microprobe instrument, 20 kV, 15 nA) for nechelyustovite. Supposing that all Al belongs to the associated natrolite with ideal composition $Na_2Al_2Si_3O_{10}{\cdot}2H_2O$, our raw chemical data were corrected by subtracting the natrolite contribution. Correction of the chemical data for the presence of lamprophyllite cannot be done due to its chemical composition close to that of nechelyustovite. The shown H_2O content is the difference to 100 % because, as mentioned above, it could not be determined by weight loss due to the scarcity of the pure sample studied by the author A.P.K. and the submicrometric intergrowth of other phases described above for the sample used in this work.

According to the general formula for the bafertisite series with $p = 0$ (see section Introduction) and using a part of Na to fill the Y site, the following crystal-chemical formulae are obtained from our analysis and that of Khomyakov (1995), in the order:

$(Ba_{0.75}Sr_{0.25}K_{0.17}Ce_{0.02}Ca_{0.01}\square_{0.80})_{\Sigma 2.00}\{(Na_{2.20}Ti_{0.94}Mn_{0.62}Ca_{0.20}Fe_{0.04})_{\Sigma 4.00}[(Ti_{1.33}Nb_{0.67})_{\Sigma 2.00}O_2Si_4O_{14}](O_{1.30}H_2O_{0.70})_{\Sigma 2.00}\}{\cdot}4.325H_2O$;

$(Ba_{0.70}Sr_{0.23}K_{0.21}Ca_{0.14}\square_{0.72})_{\Sigma 2.00}\{(Na_{2.65}Ti_{0.65}Mn_{0.61}Ca_{0.06}Fe_{0.03})_{\Sigma 4.00}[(Ti_{1.34}Nb_{0.66})_{\Sigma 2.00}O_2Si_4O_{14}](H_2O_{0.865}F_{0.61}O_{0.525})_{\Sigma 2.00}\}{\cdot}4.425H_2O$.

For these compositions and the cell parameters given above, the calculated density ($Z = 4$) is D_{calc} 3.22 and 3.18 g/cm^3 in the order; the higher density observed by Khomyakov (1995), 3.42 g/cm^3, is presumably due to the presence of

Table 2. X-ray powder diffraction data for nechelyustovite extracted from the experimental profile of Fig. 9.

$^{\$}d_{obs}$	I_{obs}	d_{calc}		hkl	
		$P2/m$	$A2/m$	$P2/m$	$A2/m$
24.06	100	24.05	24.05	001	002
12.10	13	12.02	12.02	002	004
7.99	22	8.02	8.02	003	006
7.05	9	7.00	6.97	010	011
5.95*	97	6.01	6.01	004	008
3.95$^{\times}$	6	4.04, 4.01, 4.00, 3.97	4.05, 4.01, 3.97	$\bar{1}04^{\&}$, 006, $112^{\&}$, 104	$\bar{1}08^{\&}$, $00\underline{12}$, 108
3.63*	25	3.62	3.71, 3.65, 3.62, 3.60	$\bar{1}05$	$01\underline{11}$, $\bar{1}17$, $\bar{1}0\underline{10}$, 117
3.47$^{\times}$	13	3.50, 3.48, 3.46, 3.44	3.48, 3.44	$11\bar{4}$, 016, $021^{\&}$, $007^{\&}$	$022^{\&}$, $00\underline{14}$
3.07$^{\times}$	6	3.08	3.08	017	$\bar{1}1\underline{11}$
3.01$^{\times}$	6	3.01	3.03, 3.01	008	$11\underline{11}$, $00\underline{16}$
2.828$^{\times}$	16	2.855, 2.842	2.868, 2.854, 2.840	$\bar{1}22$, 122	$\bar{1}24$, 124, $02\underline{10}$
2.773$^{\times}$	13	2.763, 2.762, 2.744	2.774, 2.755	$\bar{1}23$, 018, 123	$\bar{1}26$, 126
2.712$^{\times}$	19	2.694, 2.685	2.690, 2.679, 2.667, 2.656	$\bar{1}17$, 200	200, $20\bar{2}$, $202^{\&}$, $\bar{1}28^{\&}$
2.594*$^{\times}$	34	2.636, 2.631, 2.624, 2.601	2.645, 2.635, 2.625, 2.603	026, $20\bar{2}^{\&}$, 124, 108	$02\underline{12}$, $\bar{2}04^{\&}$, $01\underline{17}$, $10\underline{16}$
2.459*$^{\times}$	69	2.496, 2.492, 2.474, 2.469	2.511, 2.500, 2.473, 2.438	019, 125, $\bar{1}18$, $\bar{2}04$	$\bar{2}11^{\&}$, $12\underline{10}$, $\bar{2}08$, 208
2.270*$^{\times}$	31	2.280, 2.279, 2.248	2.322, 2.289, 2.286	028, $\bar{1}19$, $119^{\&}$	033, $\bar{2}19^{\&}$, $02\underline{16}$
2.155$^{\times}$	13	2.135, 2.130, 2.110, 2.108, 2.103	2.163, 2.162, 2.138, 2.137	$\bar{2}07$, $220^{\&}$, $13\bar{2}^{\&}$, 216, $22\bar{2}^{\&}$	$11\underline{19}$, $21\underline{11}$, $\bar{2}0\underline{14}$, $220^{\&}$
2.063*$^{\times}$	31	2.099, 2.088, 2.081, 2.042	2.110, 2.102, 2.096, 2.093	035, 128, $11\underline{10}$, $\bar{2}17^{\&}$	$\bar{2}24^{\&}$, $\bar{1}35$, $\bar{2}1\underline{13}^{\&}$, $12\underline{16}$
1.969*$^{\times}$	22	1.998, 1.985, 1.982, 1.957	2.004, 1.989, 1.982, 1.961	$224^{\&}$, $\bar{1}29$, $02\underline{10}$, $\bar{1}1\underline{11}$	$228^{\&}$, $\bar{1}2\underline{18}$, $03\underline{13}$, $21\underline{15}$
1.942*$^{\times}$	13	1.942, 1.937, 1.933, 1.930	1.942, 1.924	$\bar{2}18$, 225, $11\underline{11}$, $037^{\&}$	$22\underline{10}$, $13\underline{11}$

$^{\$}$The seven strongest diffractions are in bold face; their choice is based on I_{calc} of the $P2/m$ polytype because I_{obs} is affected by the presence of natrolite (*) and barytolamprophyllite ($^{\times}$).

$^{\&}$Reflections not used for cell refinements.

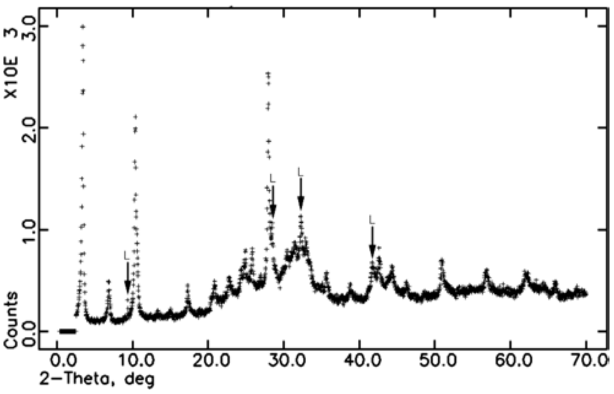

Fig. 10. Observed X-ray powder diffraction pattern of bykovaite. The most intense peaks of a labuntsovite group mineral are labelled L.

barytolamprophyllite (D_{calc} = 3.54 g/cm^3). The formula of nechelyustovite can be simplified as $(Ba,Sr,K,\square)_2\{(Na,Ti,Mn)_4[(Ti,Nb)_2O_2Si_4O_{14}](O,H_2O,F)_2\}\cdot4.5H_2O$.

Bykovaite

On the basis of the chemical data published in Khomyakov *et al.* (2005), the chemical formula of bykovaite, arranged according to the criterion used above for nechelyustovite, is $(Ba_{0.71}Na_{0.47}K_{0.12}Sr_{0.05}\square_{0.65})_{\Sigma2.00}\{(Na_{3.07}Ti_{0.61}Mn_{0.26}Ca_{0.03}Fe_{0.03})_{\Sigma4.00}[(Ti_{1.34}Nb_{0.66})_{\Sigma2.00}O_2(Si_{3.98}Al_{0.02})O_{14}]((H_2O)_{1.10}F_{0.61}OH_{0.29})_{\Sigma2.00}\}\cdot3.32H_2O$. For this composition and four formula units per unit cell in polytype $I112/m$, the calculated density is D_{calc} 2.72; the higher value of D_{obs} 2.98 is due to the presence of a labuntsovite group mineral (D_{calc} ~ 3.0) as mentioned above. The formula of bykovaite can be simplified as $(Ba,Na,K,\square)_2\{(Na,Ti,Mn)_4[(Ti,Nb)_2O_2Si_4O_{14}](H_2O,F,OH)_2\}\cdot3.5H_2O$.

Discussion

An electron diffraction study of nechelyustovite and bykovaite shows in both minerals the presence of two polytypes, 1*M* and 2*M*, which are intergrown at submicrometric scale. This type of intergrowth justifies the definition of each mineral as a species under the one root name only, without distinction between nechelyustovite-1*M* and nechelyustovite-2*M* and between bykovaite-1*M* and bykovaite-2*M*.

The chemical compositions of nechelyustovite and bykovaite are very close and, taking into account the cell parameters showing periodicities typical of the heterophyllosilicates, the corresponding crystal-chemical formulae have been constructed on the basis of the general formula of the meroplesiotype bafertisite series. On this hypothesis the same basic (*i.e.*, apart details of the conformation discussed in the section Introduction) bafertisite-type *HOH* layer is common to the structure of both minerals and the longer *c* parameter of the bykovaite polytypes must arise from differences in the interlayer space between two *HOH* layers. By comparison with anhydrous lamprophyllite, $(Sr,Ba)_2\{(Na,Ti)_4[Ti_2O_2Si_4O_{14}](OH,F)_2\}$, c = 19.22 Å (Krivovichev *et al.*, 2003) and barytolamprophyllite, $(Ba,Na)_2\{(Na,Ti)_4[Ti_2O_2Si_4O_{14}](OH,F)_2\}$, c = 19.83 Å (Peng *et al.*, 1984), one can argue that the longer *c* parameters of nechelyustovite and bykovaite are crystal-chemically related with hydration.

According to N. Chukanov (private communication) the IR data given in Table 1 are typical for bafertisite-type heterophyllosilicates. In particular, the strong band of Si–O stretching vibration (in the range 940–960 cm^{-1}) reflects the similarity of the type of condensation of SiO_4 tetrahedra in nechelyustovite, bykovaite, bornemanite and other bafertisite layer-based minerals.

The pseudomorphs after bornemanite reported by Khomyakov (1995) for bykovaite supports a genetic relationship between these two heterophyllosilicates: the latter

Table 3. Chemical composition of nechelyustovite.

Oxides (wt.%)	This paper				Khomyakov (1995)		
	Average*	Range	Minus natrolite	Standard	Average*	Range	Standard
Na_2O	14.07	13.62–15.31	7.76	Albite	9.44	9.17–9.92	Chkalovite
K_2O	0.24	0.1–0.38	0.92	Microcline	1.12	0.98–1.23	Microcline
CaO	0.35	0.16–0.50	1.34	Anorthite	1.30	1.18–1.45	Diopside
SrO	0.76	0.23–1.14	2.91	Sr-anorthite	2.75	2.71–2.88	$SrTiO_3$
BaO	3.41	1.24–4.90	13.05	Paracelsian	12.39	12.16–13.00	Barite
Ce_2O_3	0.09	0.00–0.21	0.345	REE3CHGO$^\$$	n.d.	n.d.	
FeO$^{\&}$	0.09	0.00–0.14	0.345	Ilmenite	0.27	0.20–0.30	Almandine
MnO	1.30	0.57–1.85	4.975	Hortonolite	4.97	4.56–5.30	Rhodonite
Al_2O_3	19.81	17.22–23.39		Microcline	Absent		Microcline
SiO_2	42.16	39.43–44.55	27.33	Microcline	27.60	27.03–28.76	Chkalovite
TiO_2	5.38	2.18–7.71	20.59	Ilmenite	18.30	17.72–18.95	$SrTiO_3$
Nb_2O_5	2.65	1.23–4.04	10.14	Metallic Nb	10.14	8.79–11.02	$LiNbO_3$
F	Absent			Fluorite	1.34	1.26–1.40	Fluorphlogopite
$H_2O^§$	9.69		10.295		10.94		
$-O{=}F_2$					0.56		
Total	100.00		100.00		100.00		

*Five point analyses. $^§H_2O$ calculated by difference. $^{\&}$Fe was supposed to be bivalent. $^\$$Glass containing 4.00 % of Ce_2O_3.

Table 4. Comparative characteristics of nechelyustovite and bykovaite.

Mineral	Nechelyustovite		Bykovaite	
Formula	$(Ba,Sr,K,\square)_2\{(Na,Ti,Mn)_4[(Ti,Nb)_2O_2Si_4O_{14}](O,H_2O,F)_2\}\cdot 4.5H_2O$		$(Ba,Na,K,\square)_2\{(Na,Ti,Mn)_4[(Ti,Nb)_2O_2Si_4O_{14}](H_2O,F,OH)_2\}\cdot 3.5H_2O$	
System	Monoclinic		Monoclinic	
Space group	*P*2/*m*	*A*2/*m*	*P*112/*m*	*I*112/*b*
a (Å)	5.37	5.38	5.552	5.552
b (Å)	7.00	7.04	7.179	7.179
c (Å)	24.05	48.10	25.47	50.94
	β 91.1°	91.1°	γ 91.10°	91.10°
V ($Å^3$)	905	1823	1015	2030
Z	2 for polytype *P*2/*m*		2 for polytype *P*112/*m*	
D (g/cm^3)	3.20		2.98	
Strongest XRPD lines, *d*(Å)(*I*)(*hkl*)	24.06(100)(001)* 7.05(13)(010) 5.95(36)($\underline{0}04$) 3.95(25)($\bar{1}04$, $\underline{0}06$, 112, 104) 2.828(42)($\underline{1}22$, $\bar{1}22$) 2.712(19)($\bar{1}17$, 200) 2.155(13)($\bar{2}07$,220,$13\bar{2}$,216,$22\bar{2}$)		25.24(100)(001)** 12.66(12)(002) 8.43(59)(003) 3.43(12)(022) 3.16(48)(008) 2.755(19)(108, $20\underline{1}$, 124, 026) 2.107(12)($00\underline{12}$, $2\bar{1}7$, 223, 217)	
α	1.700		1.668	
β	1.710		1.679	
γ	1.734		1.710	
2V (°)	(+) 66 (calc)		(+) 63	
Colour	Creamy		Creamy, pale yellow	

*Indices for polytype *P*2/*m*. **Indices for polytype *P*112/*m*.

could be considered a secondary hydrated phase derived from bornemanite *via* Na_3PO_4 or Na_2HPO_4 leaching and hydration. A similar mechanism could be proposed for nechelyustovite, for which however a mother bornemanite-like phase has not been observed. Nechelyustovite and its mother phase can be new examples of transformation minerals that occur in the bafertisite series and can be compared with the cases of epistolite and murmanite which, in the order, derive from vuonnemite and lomonosovite *via* Na_3PO_4 or Na_2HPO_4 leaching and hydration [Khomyakov, 1995; *cf.* also Nèmeth *et al.* (2005) for a discussion].

In conclusion, lattice parameters, IR data, chemical composition and pseudomorphosis suggest that the crystal structures of nechelyustovite and bykovaite are based on bafertisite-type *HOH* layers (Table 4). In other words, these two titano-silicates represent two new members of the bafertisite mero-plesiotype bafertisite series. In spite of the similar chemical composition, the differences in the cell parameters suggest that their crystal structures substantially differ. In particular, the monoclinic angle (~ 91°) is γ (*i.e.*, between edges ~ 5.5 and ~ 7.1 Å long, which are parallel to the *HOH* layer) in bykovaite, and β [*i.e.*, between edges ~ 5.4 and ~ 48 (or 24) Å long] in nechelyustovite; further, the lattice of the 2*M* polytype is *I* centred in bykovaite and *A* centred in nechelyustovite.

Acknowledgements: This work was financially supported by MIUR (Roma, PRIN project "Minerals to materials: crystal chemistry, microstructures, modularity, modulations"). We are grateful to I. Dódony for taking the SAED pattern of Fig. 8a and to N. Chukanov for the IR data. Comments by the referees I. Pekov and C. Viti helped to improve the presentation of the data.

References

Christiansen, C.C., Makovicky, E., Johnsen, O.N. (1999): Homology and typism in heterophyllosilicates: an alternative approach. *N. Jb. Mineral. Abh.*, **175**, 153-189.

Ferraris, G. (1997): Polysomatism as a tool for correlating properties and structure. *EMU Notes Mineral.*, **1**, 275-295.

— (2008): Modular structures – the paradigmatic case of heterophyllosilicates. *Z. Kristallogr.*, **223**, 76–84.

Ferraris, G., Ivaldi, G., Khomyakov, A.P., Soboleva, S.V., Belluso, E., Pavese, A. (1996): Nafertisite, a layer titanosilicate member of a polysomatic series including mica. *Eur. J. Mineral.*, **8**, 241-249.

Ferraris, G., Ivaldi, G., Pushcharovsky, D. Yu., Zubkova, N., Pekov, I. (2001): The crystal structure of delindeite, $Ba_2\{(Na,K,\square)_3(Ti,Fe)[Ti_2(O,OH)_4Si_4O_{14}](H_2O,OH)_2\}$, a member of the mero-plesiotype bafertisite series. *Can. Mineral.*, **39**, 1306-1316.

Ferraris, G., Belluso, E., Gula, A., Khomyakov, A.P., Soboleva, S.V. (2003): The crystal structure of seidite-(Ce), $Na_4(Ce,Sr)_2\{Ti(OH)_2(Si_8O_{18})\}(O,OH,F)_4\cdot 5H_2O$, a modular microporous titanosilicate of the rhodesite group. *Can. Mineral.*, **41**, 1183-1192.

Ferraris, G., Makovicky, E., Merlino, S. (2008): Crystallography of modular materials. IUCr/Oxford University Press, Oxford, UK, 372 p.

Holland, T.J.B. & Redfern, S.A.T. (1997): Unit cell refinement from powder diffraction data: the use of regression diagnostic. *Mineral. Mag.*, **61**, 65-77.

Khomyakov, A.P. (1995): Mineralogy of hyperagpaitic alkaline rocks. Clarendon Press, Oxford, UK, 248 p.

— (2008): The largest source of minerals with unique structures and properties. *in* "Minerals as advanced materials I", S.V. Krivovichev, ed. Springer, Berlin, 71-77.

Khomyakov, A.P., Ferraris, G., Nechelyustov, G.N., Ivaldi, G., Soboleva, S.V. (1995): Nafertisite $Na_3(Fe^{2+},F^{3+})_6[Ti_2Si_{12}O_{34}](O,OH)_7\ 2H_2O$, a new mineral with a new type of band silicate radical. *Zap. Vseross. Mineral. Obshch.*, **124**, 6, 101-108 (in Russian).

Khomyakov, A.P., Ferraris, G., Belluso, E., Britvin, S.N., Nechelyustov, G.N., Soboleva, S.V. (1998): Seidite-(Ce), $Na_4SrCeTiSi_8O_{22}F{\cdot}5H_2O$ – a new mineral with zeolite properties. *Zap. Vseross. Mineral. Obshch.*, **127**, 4, 94-100 (in Russian).

Khomyakov, A.P., Menshikov, Yu. P., Ferraris, G., Nèmeth, P., Nechelyustov, G.N. (2005): Bykovaite, $BaNa\{(Na,Ti)_4[(Ti,Nb)_2(OH,O)_3Si_4O_{14}](OH,F)_2\}{\cdot}3H_2O$, a new heterophyllosilicate from the Lovozero alkaline massif, Kola Peninsula, Russia. *Zap. Vseross. Mineral. Obshch.*, **134**, 5, 40-49 (in Russian).

Krivovichev, S.V., Armbruster, Th., Yakovenchuk, V.N., Pakhomovsky, Y.A., Menshikov, Yu. P. (2003): Crystal structures of lamprophyllite-2*M* and lamprophyllite-2*O* from the Lovozero alkaline massif, Kola Peninsula, Russia. *Eur. J. Mineral.*, **15**, 711-718.

Makovicky, E. (1997): Modularity – different types and approaches. *EMU Notes Mineral.*, **1**, 315-343.

Mandarino, J.A. (1981): The Gladstone–Dale relationship: part IV. The compatibility concept and its application. *Can. Mineral.*, **19**, 441-450.

Nèmeth, P. (2004): Characterization of new mineral phases belonging to the heterophyllosilicate series. PhD Dissertation, Dipartimento di Scienze Mineralogiche e Petrologiche, Università di Torino, Torino, Italy.

Nèmeth, P., Ferraris, G., Radnóczi, G., Ageeva, O.A. (2005): TEM and X-ray study of syntactic intergrowths of epistolite with murmanite and shkatulkalite. *Can. Mineral.*, **45**, 973-987.

Pekov, I.V. (2000): Lovozero massif: history, pegmatites, minerals. Ocean Pictures Ltd., Moscow, 480 p.

Pekov, I.V. & Podlesnyi, A.S. (2004): Kukisvumchorr deposit: mineralogy of alkaline pegmatites and hydrothermalites. Mineralogical Almanac Publishing, Moscow, 164 p.

Peng, Z.Z., Zhang, J., Shu, J. (1984): The crystal structure of barytolamprophyllite. *Kexue Tongbao*, **29**, 237-241.

Perekalina, Z.B. & Khomyakov, A.P. (1999): Diffuse reflection spectra of natural titanosilicates. *Crystallogr. Rep.*, **44**, 130-133.

Sokolova, E. (2006): From structure topology to chemical composition I. Structural hierarchy and stereochemistry in titanium disilicate minerals. *Can. Mineral.*, **44**, 1273-1330.

Yakovenchuk, V.N., Ivanyuk, G. Yu., Pakhomovsky, Ya. A., Menshikov, Yu. P. (2005): Khibiny. Laplandia Minerals, Apatity, 468 p.

Zvyagin, V.V. & Vrublevskaya, Z.V. (1976): Polytypic forms of astrophyllite. *Sov. Phys. Crystallogr.*, **21**, 542-545.

Received 5 February 2008
Modified version received 20 June 2008
Accepted 30 June 2008